Korean J. Chem. Eng., 34(6), 1619-1629 (2017)
DOI: 10.1007/s11814-017-0029-x

pISSN: 0256-1115
eISSN: 1975-7220

Technology development for the reduction of NOx in flue gas from a burner-type vaporizer and its application

Jeongeun Son*, Huicheon Yang*, Geonjoong Kim*,†, Sungwon Hwang*,†, and Hyunseok You**

*Graduate School of Chemistry and Chemical Engineering, Inha University, 100 Inha-ro, Nam-gu, Incheon 22212, Korea
**New Energy Technology Center, KOGAS Research Institute, 1248, Suin-ro, Sangnok-gu, Ansan-si, Gyeonggi-do 15328, Korea
(*Received 25 November 2016 • accepted 6 February 2017*)

Abstract−We developed a modified process of a submerged combustion vaporizer (SMV) to remove nitric oxides (NOx) efficiently from flue gas of the SMV at liquefied natural gas (LNG) terminals. For this, excess oxygen is injected into exhaust gas that contains NOx from SMV burner. Then, the mixed gas spreads into a hydrogen peroxide solution or water bath. We initially performed experiments of the modified system to estimate the effect of various process variables (temperature, excess O_2 concentration, pH of water, residence time of flue gas in water tank, and H_2O_2 concentration) on NOx conversion, and developed a mathematical model of the system based on the experiment results. Lastly, we confirmed higher performance of the modified system and validated the feasibility for its field application.

Keywords: deNOx, Modeling, Optimization, Submerged Combustion Vaporizer, Kinetic

INTRODUCTION

The exhaust gas discharged from combustion processes includes a variety of different types of air pollutants and hazardous compounds. In particular, nitrogen oxides (NOx=NO, NO_2, N_2O, N_2O_3, N_2O_4, N_2O_5) are well-known air pollutants. Among them, nitrogen oxide and nitrogen dioxide are the most common nitrogen oxides in the atmosphere. Pollutants from power plants and industrial boilers are highly toxic for humans, and they participate in the formation of photochemical smog. Furthermore, they are one of the sources to produce particulate matters in the atmosphere. Thus, this research focuses on the control of NOx emission from combustion processes such as SMVs (submerged combustion vaporizers) at LNG (liquefied natural gas) terminal.

Nitrogen oxides are mainly produced from combustion, with power, heat engineering facilities and transporters are the major contributors of these pollutants. Table 1 illustrates the amount of nitrogen emissions from various sources [1]. Note that total emissions from industry have decreased over the past few years. NOx emissions from combustion in the energy and transformation industries have substantially decreased. In addition, we are expecting that NOx emission will decrease further thanks to combustion technology improvement. Furthermore, NOx regulations will be restricted more and more around the world to prevent NOx generation [2]. For example, in Europe, EURO 6 has been implemented since 2014 to reduce air contaminants discharged from vehicles. Similarly, pollutant load management for industrial fields, a proactive method to manage total emissions, has been conducted in South Korea. For these reasons, improvement of NOx reduction technology is vital to prepare for these restrictions in the near future.

Table 1. Emissions of nitrogen oxides in South Korea as NO_2

Emission sources	2003	2006	2009	2012
		[t·yr^{-1}]		
Combustion in energy and transformation industries	396,070	364,310	143,274	169,346
Non-industrial combustion plants	94,602	89,127	86,636	87,935
Combustion in the manufacturing industry	123,221	101,197	159,511	172,761
Production processes	53,664	56,577	41,409	59,002
Road transport	472,245	450,080	368,048	345,666
Other mobile sources and machinery	203,583	196,441	207,829	225,561
Waste treatment and disposal	18,755	17,237	7,426	14,782
Other sources and sinks	-	-	185	154
Total	1,362,140	1,274,969	1,045,103	1,075,207

†To whom correspondence should be addressed.
E-mail: sungwon.hwang@inha.ac.kr, kimgj@inha.ac.kr

Numerous technologies have been developed to reduce NOx emissions, and they belong to one of three types: pre-treatment, combustion modification, and post-treatment process. Pre-treatment is a preventive technique that reduces NOx generation before combustion. The feed materials, such as fuel and oxidizer (including nitrogen components), are treated to reduce NOx formation. Combustion modification minimizes NOx formation by modifying the combustion process. Several methods, such as low NOx burners (LNB), low excess air (LEA), and flue gas recirculation (FGR), have been considered for the modification of the combustion process. However, these processes may reduce the thermal efficiency of the combustion process and increase carbon monoxide formation. The post-treatment process reduces NOx from exhaust gases by using certain chemical and physical treatments, such as catalytic reduction (selective catalytic reduction (SCR), selective non-catalytic reduction (SNCR)), adsorption, and absorption. Although post-treatment processes have higher NOx removal efficiency and productivity than the other NOx removal methods, they are capital-intensive, and thus require sufficient feasibility study for field applications.

Vaporizers, such as ORVs (open rack vaporizers) and SMVs, are normally used to vaporize LNG to natural gas. SMVs use natural gas as fuel for the burner, and the amount of NOx discharged from the SMV stack is currently restricted to 50 ppm. Fig. 1 shows a schematic diagram of an SMV. The combustion gas is generated from the burner, which heats the water in the water bath. LNG is then vaporized inside tubes through heat exchange from the heated water. ORVs are commonly utilized at LNG terminals to supply natural gas. Meanwhile, SMV is used when the demand for natural gas goes beyond the capacity of ORVs, or the production capacity is reduced by a low water temperature during the winter. A portion of the NOx from the flue gas is absorbed into the water, and the rest is discharged to atmosphere.

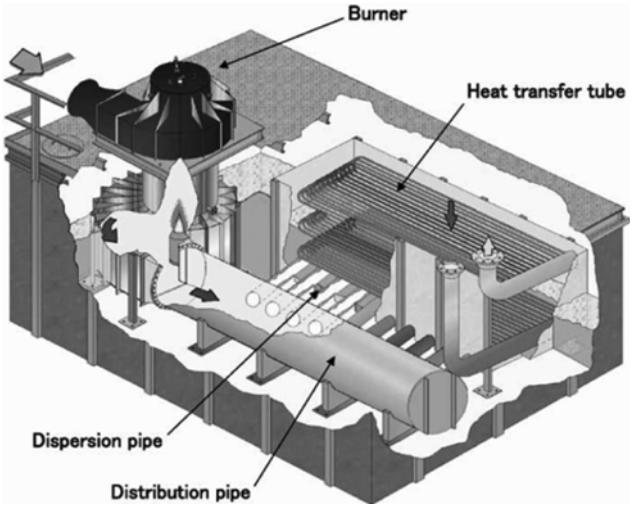

Fig. 1. Schematic diagram of a submerged combustion vaporizer (SMV) [3].

In Korea, KOGAS (Korea Gas Corporation, headquartered in Incheon and Pyeongtaek, Korea) was recently classified as the first-class discharger since 2015 in accordance with a revised Clean Air Conservation Act. Accordingly, NOx in the exhaust gas discharged from the SMV is now regarded as one of major pollutants, which has been restricted by regulation. Therefore, we planned to mitigate the discharged amount of NOx. The exhaust gas emitted from SMV has a temperature range of 298 to 303 K. The operating temperature is too low to adopt post treatment technologies such as SCR or SNCR that require much higher temperature for activation of reactions to remove NOx. In fact, there has not been much requirement in industry to remove NOx from flue gas at low-temperature for a large capacity, in particular using SMVs. Furthermore, KOGAS has dozens of these SMVs at each field of LNG terminals. Thus, our research focused on developing a new technology to remove NOx from the flue gas at low temperature with less capital investment to achieve economic feasibility.

After considering several technical alternatives and their economic feasibility, we devised a system to inject additional oxidants (oxygen, hydrogen oxide) into flue gas after combustion, and to distribute the flue gas at the bottom of a water bath as bubbles. In this way, NO can be converted to NO_2 that is more soluble and absorbed in water, diluted by H_2O_2 (Table 2). The pH of water becomes lower due to generation of acids throughout the reaction. So, the acidity of water should be controlled to maximize the NOx removal efficiency.

To prove the efficiency and find an optimum operating condition of a newly developed system, we set the experiments at a small scale. First, the oxidation of NO and absorption of NO_2 in water bath were conducted under various operating conditions, and the concentration of NOx that was discharged from the bath was measured. Secondly, the system was mathematically modeled based on the experimental results, and the final NO conversions were predicted based on different values of process variables (temperature, excess O_2 concentration, pH of water, residence time of flue gas in water tank, and H_2O_2 concentration). Lastly, the parameters of the reaction system were fitted to minimize the differences between the experimental and calculated results to increase accuracy of the model. The model allows us to evaluate a newly developed sys-

Table 2. Classification and characteristics of nitrogen oxides [4]

Formula	Name	Nitrogen valence	Physical properties	Henry constant
N_2O	Nitrous oxide	1	Colorless gas, water soluble	
NO	Nitric oxide	2	Colorless gas, slightly water soluble	$K_H=1.9\times10^{-3}$ mol·atm^{-1}
N_2O_3	Dinitrogen trioxide	3	Black solid, water soluble, decomposes in water	
NO_2	Nitrogen dioxide	4	Red-brown gas, very water soluble, decomposes in water	$K_H=1.0\times10^{-2}$ mol·atm^{-1}
N_2O_5	Dinitrogen pentoxide	5	White solid, decomposes in water	

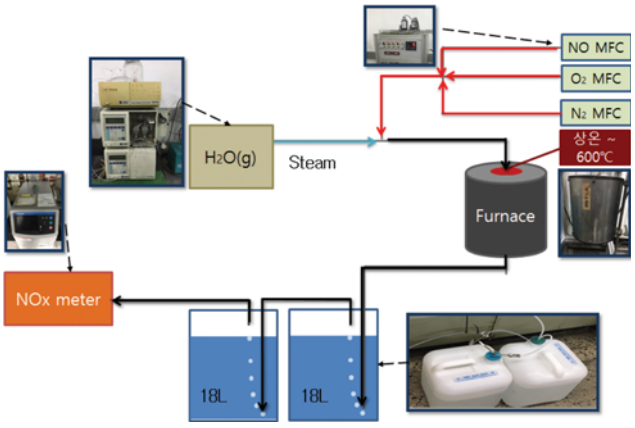

Fig. 2. Schematic diagram of the apparatus used for the experiments.

tem more effectively in terms of economic feasibility, operability and potential scale-up issues.

RESEARCH METHODS

1. Experimental Setting

The configuration of experimental apparatus setting is shown in Fig. 2. Feeds of O_2 (99.5%), NO (0.1% NO, 99.9% N_2) and N_2 (99.995%) are injected separately and merged into a stream (red line) using a mass flow controller (MFC, Brooks). The stream is then mixed with steam, and the mixed gas is injected to a furnace for combustion (black line), where its temperature is controlled. The experiments were conducted both in the presence and absence of steam to compare the effect of water vapor on the oxidation of NO (actual exhaust gas contains 12-13% steam). The steam was supplied by a liquid chromatography pump at a constant flow rate (0-10 $mL \cdot min^{-1}$). The flue gas after combustion was distributed at the bottom of water bath through the branches of distributor, where the reaction and absorption of NOx mainly occurred. For reference, the water contained 0-3% of aqueous H_2O_2 solution. Lastly, a NOx analyzer (Horiba Co., APNA-370) examined the gas at the outlet of the water bath.

Approximately 30-40 minutes was required to obtain reliable and stable measurements. The NO oxidation and NO_2 absorption experiments were conducted separately under different values of process variables (flow rate, temperature, excess oxygen concentration, residence time, H_2O_2 concentration, and pH) as shown in Table 3.

2. Mathematical Modeling

The modified SMV process includes injection of extra O_2 to flue gas after combustion and absorption NOx in water bath that contains a portion of H_2O_2. To develop a mathematical model of the modified SMV system, both NO oxidation in gas phase as a post-combustion process and NO absorption process in aqueous phase that occurs in a water bath are considered in the following two sections.

2-1. NO Oxidation in Gas Phase

Studies of the basic chemical kinetics for the oxidation of NO by O_2 in gas phase and liquid phase have been performed over the past few years [5-21]. The reaction mechanism and rate constants were investigated by Morrison et al. [5] as follows:

$$2NO_2 \leftrightarrow N_2O_4 \ (K_2) \quad (1)$$

$$NO + O_2 \leftrightarrow NO_3 \ (K_3) \quad (2)$$

$$NO + NO_2 \leftrightarrow N_2O_3 \ (K_4) \quad (3)$$

$$N_2O_3 + O_2 \leftrightarrow N_2O_5 \ (K_5) \quad (4)$$

$$N_2O_5 \rightarrow NO_2 + NO_3 \ (k_6) \quad (5)$$

$$NO + NO_3 \rightarrow 2NO_2 \ (k_7) \quad (6)$$

Intermediates, such as NO_3, N_2O_3, and N_2O_5, are included in the following reaction mechanism. This reaction is described with the second order in nitric oxide and the first order in oxygen [6]:

$$2NO + O_2 = 2NO_2 \quad (7)$$

$$-\frac{d[NO]}{dt} = +\frac{d[NO_2]}{dt} = 2k \cdot [NO]^2 \cdot [O_2] \quad (8)$$

The chemical kinetics of this reaction was first studied by Bodenstein and Wachenheim [7]. Since then, many investigators have studied the reaction system, as shown in Table 4 [5,8-21]. The results show experiment data under low NO concentrations (ppm). In addition, the data shows that reaction rate generally decreases with respect to temperature increase either at ambient or subzero temperature. It proves that the temperature coefficient is negative

Table 3. Experimental conditions

	Experimental conditions	SMV (Spec.)
Temperature of flue gas	298-873 K	>1273 K
Content of water vapor in flue gas		12-13%
NOx (ppm) of flue gas	50-500 ppm	
Volumetric flow rate of flue gas	N_2 2850 $mL \cdot min^{-1}$ (298 K, 1 atm)	Fuel gas 2530 $Nm^3 \cdot h^{-1}$
	O_2 100 $mL \cdot min^{-1}$	Air 24095 $Nm^3 \cdot h^{-1}$
	NO 50 $mL \cdot min^{-1}$	
NOx of exhaust gas from stack (ppm)		50 ppm
O_2 of exhaust gas from stack		4%
Amount of water in the water bath	18-54 L	62.4 m^3 (62,400 L)
Temperature of the water bath	298 K	298 K
Concentration of H_2O_2	1-3%	0%

Table 4. Rate constants for the reaction $2NO+O_2=2NO_2$ in gas phase [6]

Reference	$[NO]_0$ (mol·L^{-1})	$[O_2]_0$ (mol·L^{-1})	Rate constant, k (L^2·mol^{-2}·s^{-1})	Temperature (K)
Morrison et al. [5]	9.0×10^{-8}-3.1×10^{-6}	1.3×10^{-3}-1.0×10^{-2}	4.5×10^{3}-1.1×10^{3}	290-311
Bodenstein and Wachenheim [7]	4.5×10^{-4}-8.0×10^{-4}	1.4×10^{-4}-7.3×10^{-4}	4.5×10^{3}-8.9×10^{3}	273-363
Tipper and Williams [8]	5.5×10^{-4}-5.5×10^{-3}	1.0×10^{-4}-4.9×10^{-3}	1.6×10^{3}-7.8×10^{3}	293-843
Treacy and Daniele [9]	5.4×10^{-4}	2.7×10^{-4}-1.1×10^{-3}	3.8×10^{3}	298
Mahenc et al. [10]	4.0×10^{-4}-1.0×10^{-3}	4.5×10^{-4}-8.0×10^{-4}	5.4×10^{3}-8.9×10^{3} [$5.0\times10^{2}\times0^{339/T}$]	274-333
Hisatsune and Zafonte [11]	3.1×10^{-4}-1.4×10^{-2}	4.5×10^{-4}-8.0×10^{-4}	$3.8\times10^{3}\times10^{81/T}$	277-329
Olbregts [12]	9.0×10^{-5}-1.2×10^{-3}	1.2×10^{-5}-1.4×10^{-3}	3.0×10^{3}-2.1×10^{4} [$10^{(-.18+2.70\log(T)+700/T)}$]	225-760
Smith [13]	5.9×10^{-5}-2.7×10^{-3}	1.7×10^{-4}-1.4×10^{-3}	4.9×10^{3}-7.4×10^{3}	298
Cueto and Pryor [14]	3.9×10^{-5}	8.6×10^{-3}	6.7×10^{3}	296
Brown and Crist [15]	1.1×10^{-6}-6.8×10^{-6}	4.2×10^{-4}-1.2×10^{-3}	6.8×10^{3}-7.8×10^{3}	298
Greig and Hall [16]	1.1×10^{-6}-2.2×10^{-6}	2.7×10^{-5}-1.3×10^{-2}	6.8×10^{3}-1.1×10^{3}	293-372
Greig and Hall [17]	6.9×10^{-7}-3.1×10^{-6}	7.4×10^{-3}	9.6×10^{3}-1.1×10^{3}	293
Aida et al. [18]	4.1×10^{-7}-6.5×10^{-6}	8.3×10^{-3}-4.0×10^{-2}	7.3×10^{3}-8.4×10^{3}	298-310
Stedman and Niki [19]	2.0×10^{-7}-4.1×10^{-5}	2.7×10^{-3}-3.5×10^{-2}	7.2×10^{3}	298
Bufalini and Stephens [20]	1.3×10^{-7}-8.1×10^{-7}	8.6×10^{-3}	9.0×10^{3}	299
Glasson and Tuesday [21]	8.2×10^{-8}-2.1×10^{-6}	8.2×10^{-4}-2.5×10^{-2}	6.0×10^{3}- 8.5×10^{3}	296

over a wide range of temperatures.

The mechanism and kinetics derived by Morrison et al. [5] were adopted to model the oxidation of NO in gas phase in this research because the concentration of NOx discharged from the SMV was relatively low (approximately 50 ppm). The results from the kinetics were found to be very similar to those of other investigators.

It is assumed that reactions (1) to (4) are in rapid equilibrium, and (5) to (6) occur at a measurable rate. The intermediates (NO_3, N_2O_3, and N_2O_5) were observed, and were postulated in previous studies, supporting the validity of these reaction schemes. The rate expression for the oxidation of NO derived from reactions (1) to (6) is shown on the paper by Morrison and coworkers [5]:

$$-\frac{d[NO]}{dt}=2k_7K_3[NO]^2[O_2]+k_6K_4K_5[NO][NO_2][O_2] \quad (9)$$

The concentration change with respect to time or conversion of the reaction can be calculated according to Eq. (9), where [NO], [NO_2], and [O_2] indicate the concentrations of each (mol·L^{-1}). The rate is influenced by the concentration of NO_2. K_3, K_4, and K_5 are the equilibrium constants, and k_6 and k_7 are the rate constants for each reaction. The values for $2k_7K_3$ and $k_6K_4K_5$ are 1.313×10^4 L^2·mol^{-2}·s^{-1} and 1.276×10^4 L^2·mol^{-2}·s^{-1}, respectively [5].

In addition, the actual exhaust gas discharged from the SMV contains methane, nitrogen, and water vapor; the effects of these components on the reaction of NO and O_2 were investigated. However, the rate constant was not affected by moisture or the other components [6,7,9,18]. The water reacted with NO_2, while water did not react with NO in absence of oxidant.

2-2. NO Oxidation in Liquid Phase

The process of SMV has a very small residence time. Therefore, NO oxidation in liquid phase is more dominant than in gas phase. This reaction mechanism and kinetics were established as shown in Eqs. (10) and (11) by Pogrebnaya et al. [22]. The reaction of NO oxidation to NO_2 in aqueous solution is expressed in the second order with nitric oxide and the first order in oxygen. The kinetic expression is equal to that in gas phase, while its rate constant is about 1,000 times faster than that in gas phase.

$$4NO+O_2+2H_2O\rightarrow4H^++4NO_2^- \quad (10)$$

$$\frac{d[NO_2^-]}{dt}=k_1\cdot[NO]^2\cdot[O_2] \quad (11)$$

In this research, the detailed kinetic scheme proposed by Lewin and Deen [23] was used:

$$2NO+O_2\rightarrow2NO_2(k_1) \quad (12)$$

$$NO+NO_2\leftrightarrow N_2O_3(k_2, k_3) \quad (13)$$

$$N_2O_3+H_2O\rightarrow2H^++2NO_2^-(k_4) \quad (14)$$

The kinetic expressions based on the kinetic scheme are:

$$R_{NO}=-2k_1[NO]^2[O_2]-k_2[NO][NO_2]+k_3[N_2O_3] \quad (15)$$

$$R_{O2}=-k_1[NO]^2[O_2] \quad (16)$$

$$R_{NO_2}^-=2k_4[N_2O_3] \quad (17)$$

where, R_i (i=NO, NO_2, N_2O_3) is the volumetric rate of formation and [NO], [NO_2], [O_2], and [N_2O_3] indicate the concentrations of each component. According to Lewin and Deen [23], k_1, k_2, k_3, and k_4 in reaction schemes (12)-(14) are rate constants for each reac-

Table 5. Rate constants for the reaction $2NO+O_2=2NO_2$ in liquid phase [23]

Reference	k_1 (10^6 L^2·mol^{-2}·s^{-1})			E_{act} (kcal·mol^{-1})
	288 K	295-298 K	308-310 K	
Pogrebnaya et al. [22]	1.9±0.1	2.2±0.1		2.8
Lewin et al. [23]		2.1±0.4	2.4±0.3	2.0
Wink et al. [24]		1.5±0.4	0.9±0.2	−6.5
Awad et al. [25]	1.9	2.1	2.2	1.0

tion and are 2.1×10^6 $L^2\cdot mol^{-2}\cdot s^{-1}$, 1.1×10^9 $L\cdot mol^{-1}\cdot s^{-1}$, 3.7×10^4 s^{-1}, and $0.03\times k_3$, respectively. The values of k_1 have been studied by other investigators, as shown in Table 5.

$[NO_2]$ and $[N_2O_3]$ are expressed by the concentration of NO. Each component is present in a marginal amount; thus, the mass-balanced equation of the system can be illustrated as:

$$\frac{d[NO]}{dt} = -4k_1[NO]^2[O_2] + \left(\frac{k_G A_G}{V}\right)_{NO}([NO]^* - [NO]) \quad (18)$$

where, k_G and A_G are the mass transfer coefficient in liquid phase and surface area, respectively, and mass transfer of NO and O_2 across gas-liquid interface is expressed with ($k_GA_G/V=7.3\times10^{-4}$ s^{-1}). $[NO]^*$ is the saturated nitric oxide concentration in equilibrium with its gas phase concentration.

It is difficult to increase the removal efficiency of nitric oxide, which has a low solubility in wet process that uses water as the medium. For the removal of NOx from the exhaust gas discharged from various stationary sources, such as power plants, steel pickling plants, or other plants that include combustion processes, several different solutions (sodium sulfite, sodium hypochlorite, hydrogen peroxide) have been studied by investigators [26-29]. The use of H_2O_2 as a medium in the wet process was found to be suitable for the SMV system with the withdrawal of nitric acid that is produced from the process. In theory, H_2O_2 reacts with both nitric oxide and nitrogen dioxide to form nitrous acid and nitric acid. Nitric oxide has a low solubility and reactivity in water, and a relatively high solubility and reactivity in H_2O_2. The presence of H_2O_2 in the NOx absorption process could be beneficial to the oxidation system [29-31]:

$$2NO + 2H_2O_2 \rightarrow 2NO_2 + 2H_2O \quad (19)$$

$$2NO_2 + H_2O_2 \rightarrow 2HNO_3 \quad (20)$$

The overall reaction can be represented as:

$$2NO + 3H_2O_2 \rightarrow 2HNO_3 + 2H_2O \quad (21)$$

The ratio of NO conversion or NO removal was estimated for each experiment by:

$$\text{Conversion of NO (\%)} = \frac{[NO]_i - [NO]_f}{[NO]_i} \times 100 \quad (22)$$

where, $[NO]_i$ and $[NO]_f$ are the initial and final concentrations of the system. All the experimental results were obtained after 30-40 minutes after the system becomes stable.

2-3. Modeling the Reaction System

As shown in Fig. 1, the water bath, where the reaction occurs, is a multiphase reactor to mix the gas-phase with the liquid-phase. In gas phase, the feed is injected, passes through the reactor, and is then discharged; in liquid phase, there is no inlet and outlet, and accumulation rate of NO of the system changes by the mass transfer and hydrodynamic effects. The equilibria between gas phase and liquid phase in the system are exhibited in Fig. 3. There are various forms of NOx in each phase; the equilibria relationships are formed by the non-reactive partitioning of a solute, as described by Henry's law [32]. In this research, the modified SMV system was modeled as a PFR (plug flow reactor) that includes the mass transfer impact between gas and liquid phases.

After modeling the reaction system, the parameters were estimated using MATLAB software. Parameter estimation plays a significant role in modeling the behavior of a system mathematically. It is a process to augment the accuracy and reliability of the model by minimizing the difference between the calculated and experimental values [33]. We used fifteen data sets to fit each reaction parameter, and each set was obtained at steady-state condition. The objective function, F, was used for optimization in this procedure, and is expressed as:

$$F_{obj} = \Sigma_{i=1}^{N_{resp}} \Sigma_{j=1}^{N_{exp}} (y_{exp,\,i} - y_{cal,\,i})^2 \quad (23)$$

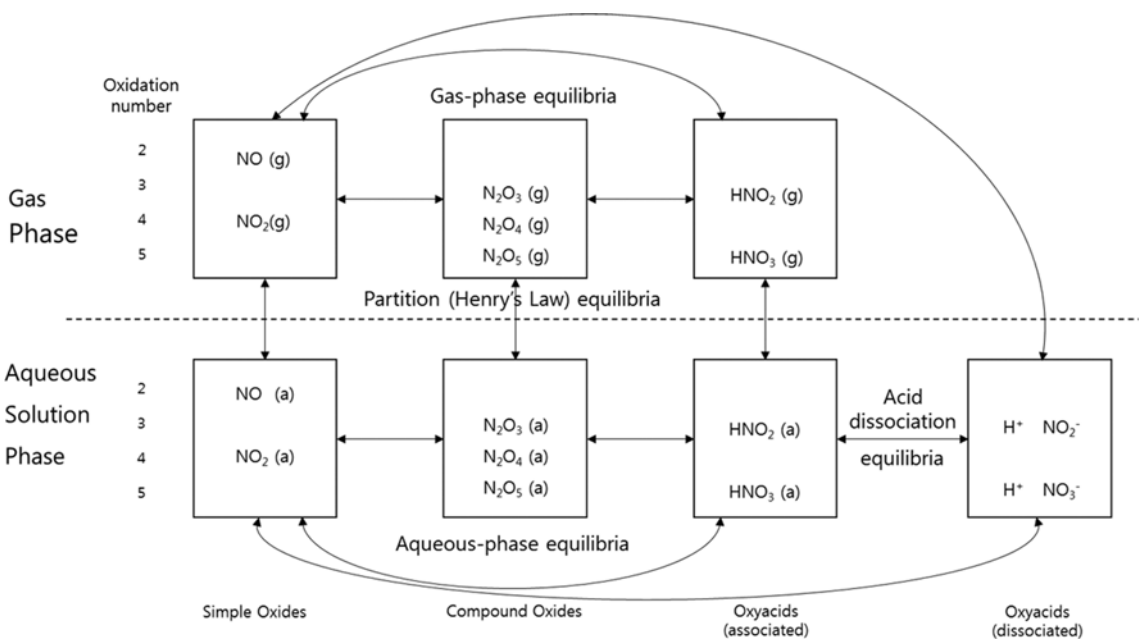

Fig. 3. Equilibria relating the gaseous and aqueous nitrogen oxides and oxyacids [32].

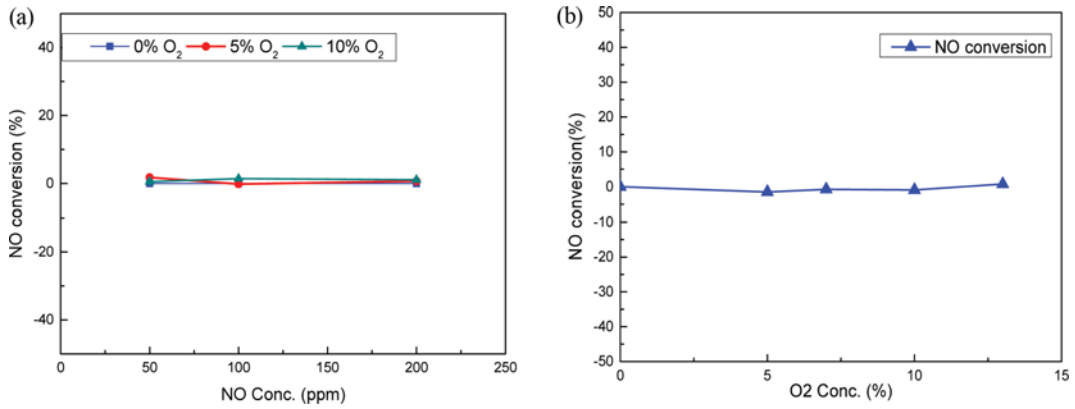

Fig. 4. Conversion of NO to NO_2 (flow rate=2 L·min^{-1}, 298 K): (a) Effect of the O_2 and NO concentration and (b) Effect of the O_2 concentration in the presence of steam at a NO concentration of 50 ppm.

where, $y_{exp,i}$ and $y_{cal,i}$ represent the experimental and calculated results for component i for the jth experiment. N_{resp} and N_{exp} are the number of species in the system and experimental runs, respectively.

RESULTS AND DISCUSSION

1. Experimental Results for NO Oxidation in Gas Phase

The results and conditions of the experiments for NO oxidation in gas phase are shown in Fig. 4. These experiments were conducted under various operating conditions (change of flow rate, temperature, NO concentration, and O_2 concentration). Fig. 4(a) indicates the conversion of NO with respect to change of the O_2 concentration at a flow rate of 2 L·min^{-1}, temperature of 298 K, and NO concentration of 50 ppm. The extra experiments were conducted by varying the O_2 concentration and temperature at a flow rate of 2 L·min^{-1} and NO concentration of 50 ppm, and injecting water vapor into the existing exhaust gas at 10 mL·min^{-1}, as shown in Fig. 4(b), to scrutinize the effect of water vapor in the actual exhaust gas on NO oxidation. The conversion of nitric oxide to nitrogen dioxide was found to be almost negligible in gas phase regardless of the NO concentration, O_2 concentration, and temperature. Meanwhile, the water vapor content in the actual exhaust gas from the SMV was approximately 12-13 vol%. Despite the high equilibrium conversion for the reaction, such low conversion rate of NO indicates that these results might be due to the characteristics of the SMV process (short contact time).

2. Experimental Results for NO Oxidation in Liquid Phase

The conditions and results for the NO oxidation experiments in liquid phase are shown in Fig. 5. These experiments were conducted at various operating conditions (change of flow rate, temperature, NO concentration, O_2 concentration, volume of the water bath). As noted, NO oxidation in aqueous phase is relatively faster than that in gas phase, which was confirmed by the experimental results at each condition.

The graph in Fig. 5(a) is in the form of a parabola, which shows that the reaction was composed of more than one primary reaction. The higher oxygen concentrations increased the conversion of NO in the presence and absence of H_2O_2 in the water bath, as shown in Fig. 5(b). In the absence of oxygen, nitric oxide was hardly converted to nitrogen dioxide in water without H_2O_2; however, about 6.9% of the nitric oxide was converted to nitrogen dioxide in water diluted by H_2O_2, which means that H_2O_2 reacted with NO. Fig. 5(c) indicates the conversion of NO with respect to the flow rate at 50 ppm NO and 10 vol% of O_2 at room temperature of 298 K. Its conversion tends to increase for a while and decrease at one point with a flow rate of 2 L·min^{-1}. This is expected to affect the contact time and the bubble flow of gas mixture in the water bath. Fig. 5(d) and (e) indicate that the conversion corresponds to the volume of the water bath at the flowrate of 2 L·min^{-1}, NO concentration of 50 ppm, 10 vol% O_2, and room temperature in the water bath and 1% H_2O_2 bath, respectively. As the volume of the water bath increases, the conversion of NO increases linearly. This is due to the increased contact time of the mixed gas with water in the bath, caused by the increased volume of the water bath. The conversion in the bath with H_2O_2 was about 1.3-times higher than the conversion in the water bath.

To investigate the effect of the H_2O_2 concentration, 1% and 3% H_2O_2 solutions were prepared, and experiments were performed in the same manner as for the water bath. The conversion was not affected in the range of 1-3% H_2O_2, as shown in Fig. 5(f). The graph in Fig. 5(g) shows the experimental results for the reaction in the presence of sodium hydroxide and sodium hypochlorite. According to Kuropka [34], the absorption of nitrogen oxides in an alkaline solution of sodium hypochlorite and sodium hydroxide provided a high removal efficiency but did not show any difference compared to our results in water without any additives. In addition, the NO conversion with respect to pH was investigated (Fig. 5(h)). As the pH decreased, the NO conversion increased, which shows the same tendency as that observed by Pires [35]. The conversion rate was relatively high at pH 1-4 but slowly decreased with respect to increase of pH. Finally, 1% H_2O_2 solution at pH 1.5 was prepared. There was a higher removal efficiency (by about 45%) at an initial NO concentration of 500 ppm. That is, the conversion of NO to NO_2 was the highest in the H_2O_2 bath at a low pH.

3. Development of Mathematical Model and Analysis of the Results

3-1. Assumptions of the Model

The experimental apparatus was modeled in the same configu-

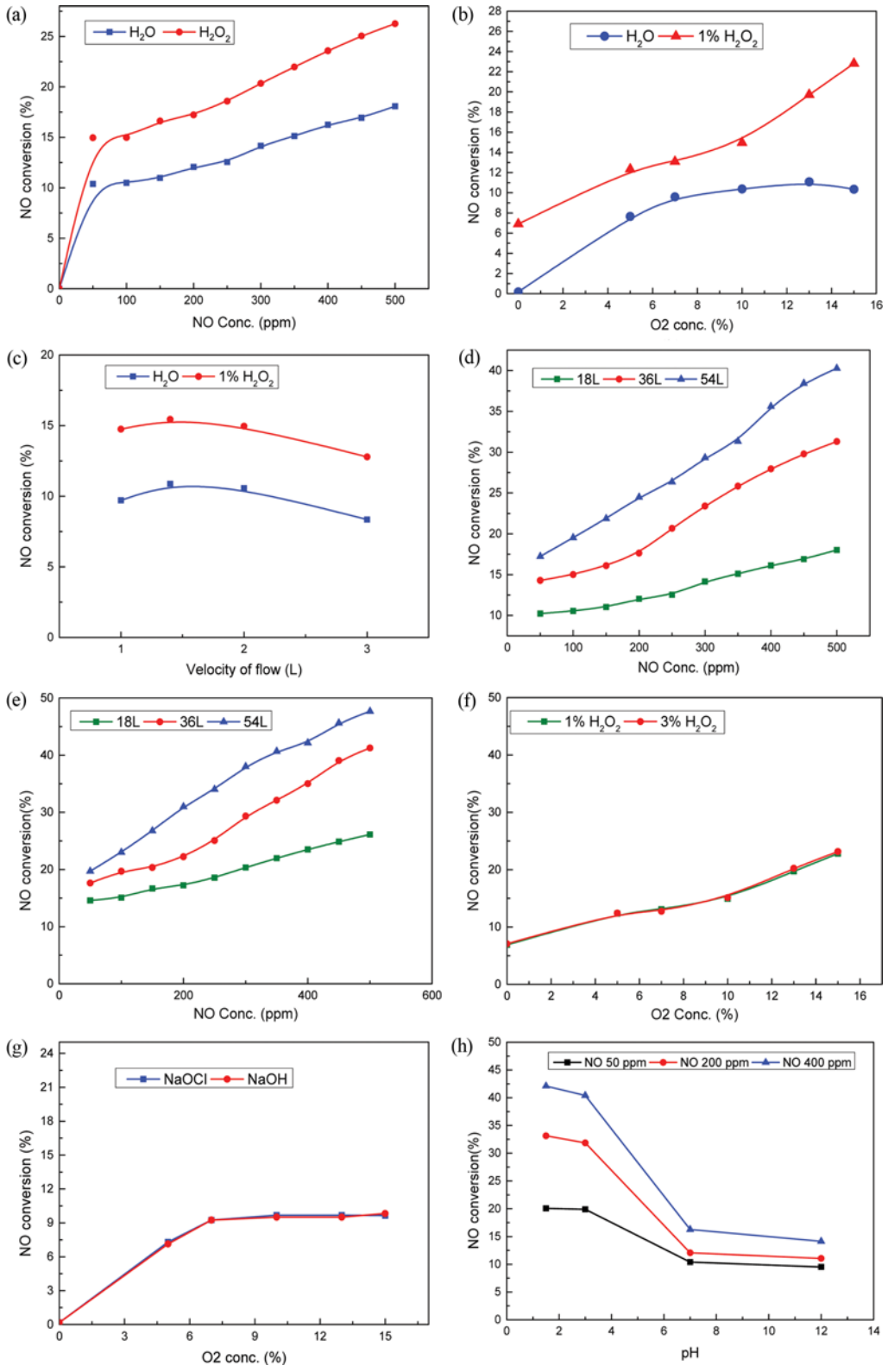

Fig. 5. Absorption ratio of NO (298 K): (a) Effect of the NO concentration with water and H_2O_2 at a flow rate of 2 L·min^{-1} and 10 vol% O_2, (b) Effect of the O_2 concentration with water and H_2O_2 at a flow rate of 2 L·min^{-1} and 50 ppm NO, (c) Effect of the flow rate with water and H_2O_2 at a 50 ppm NO and 10 vol% O_2, (d) Effect of the water bath volume and NO concentration at a flow rate of 2 L·min^{-1} and 10 vol% O_2, (e) Effect of the H_2O_2 bath volume and NO concentration at a flow rate of 2 L·min^{-1} and 10 vol% O_2, (f) Effect of the H_2O_2 concentration and O_2 concentration at a flow rate of 2 L·min^{-1} and 50 ppm NO, (g) Effect of the O_2 concentration with sodium hypochlorite and sodium hydroxide at a flow rate of 2 L·min^{-1} and 50 ppm NO, and (h) Effect of the pH and NO concentration at a flow rate of 2 L·min^{-1} and 10 vol% O_2.

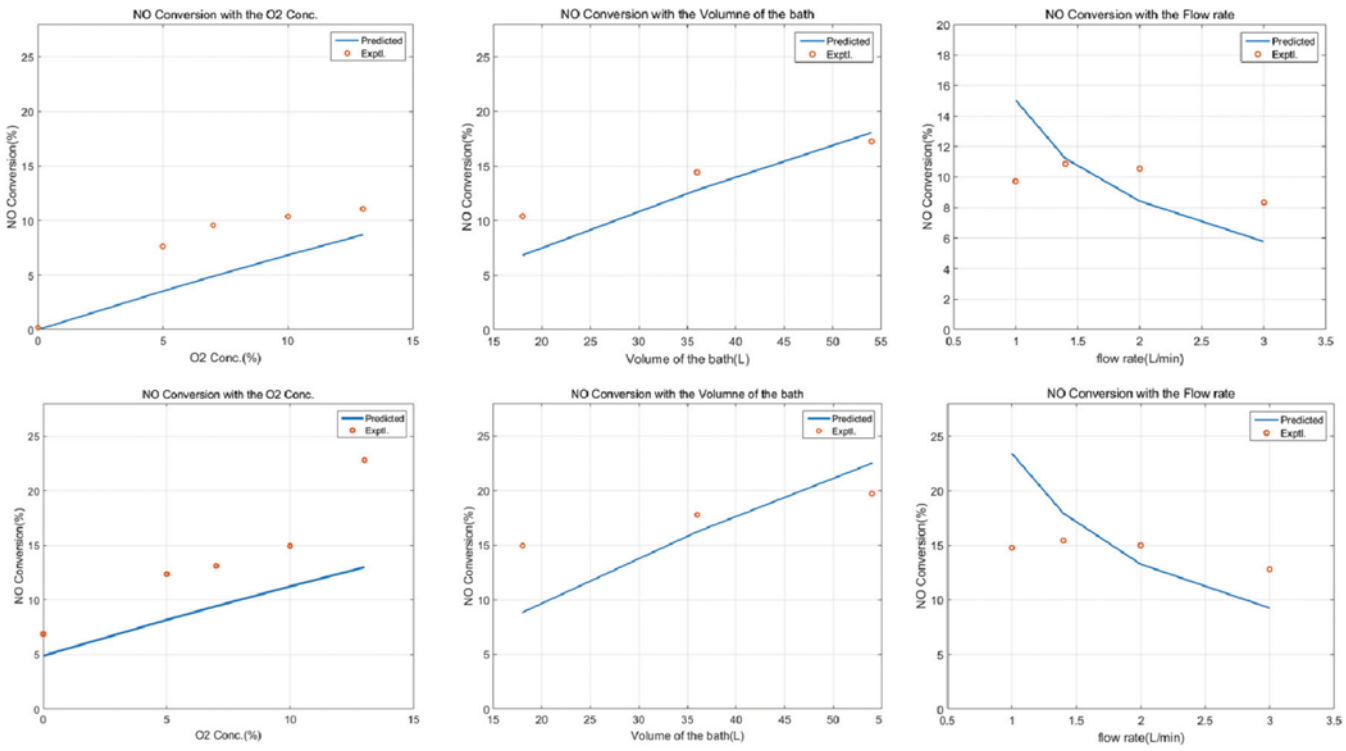

Fig. 6. Effect of oxygen concentration, flow rate, and volume of the bath in the aqueous phase.

ration as that in the SMV reaction system. The modeling was performed to verify the feasibility of this approach for field applications. Several assumptions were applied: (i) the radial flow was considered to be marginal, (ii) the Zeldovich mechanism for thermal NOx formation was ignored, (iii) the post-combustion NO concentration was 50 ppm, (iv) the effect of pressure was excluded, (v) the amount by which the combustion process heated the water was the same as the heat of vaporization for the LNG processes, and (vi) the temperature of the water bath was constant.

3-2. Modeling Results for NO Oxidation

NO oxidation to NO_2 in gas phase is described as the second order in nitric oxide and the first order in oxygen. The reaction rate decreases as the temperature increases. Eq. (9), which is based on the kinetics of the reaction mechanism that includes NO_3, N_2O_3, and N_2O_5 as intermediates, was used to model the system. The conversion of NO was predicted at various operating conditions (of concentration of O_2, concentration of NO, and the flow rate). However, the effects of various conditions on the reaction of the gas remained as almost 0% as described earlier. These results have a different tendency from NO oxidation at equilibrium conditions. The reaction rate decreased if the initial concentration of NO was low because of the reaction orders. These results are reasonable because the SMV system has a short residence time. In addition, the kinetics and mechanism in the presence of steam were investigated, and the results also showed no further impacts on the reaction, which is the same as the experimental results.

NO oxidation in aqueous phase is described in the second order with respect to nitric oxide and the first order with respect to oxygen. The rate constant for the oxidation of nitric oxide in liquid phase is about 1,000 times higher than that in gas phase. The kinetics of the reaction mechanism that includes NO_2, HNO_2, and NO_3 as intermediates (Eqs. (15) to (18)) was indicated in Eq. (24). In the mathematical model, the concentrations of NO_2 and N_2O_3 are expressed as the concentration of NO:

$$\frac{d[NO]}{dt} = -2k_1[NO]^2[O_2] - k_2[NO][NO_2] + k_3[N_2O_3] - \left(\frac{k_G A_G}{V}\right)_{NO}([NO]^* - [NO]) \quad (24)$$

The results of the experiments and modeling of the liquid NO oxidation reaction are compared in Fig. 6. The NO conversion increased with respect to the oxygen concentration, while the NO conversion decreased when the flow rate was reduced. The experimental results showed that the NO conversion increased by 17% in an oxygen range of 0-13%, flow rate of 1-3 $L \cdot min^{-1}$, and volume of 18-54 L, which was consistent with the modeling results. However, when additional air or oxygen only was injected, an insignificant NOx conversion rate was expected for the application to SMV. According to the experimental and modeling results, there was no substantial change in the NOx conversion at oxygen concentrations of 10% or more when the O_2 concentration was increased. An additional method was required for a large reduction compared to the existing NOx conversion because the oxygen content in the exhaust gas that was discharged from the stack in the SMV was about 4%.

The injection of H_2O_2 into the solution accelerated the NO oxidation reaction, which increased the conversion. The oxidation reaction of NO by H_2O_2 was shown in the first order with respect to both NO and H_2O_2, and the second order in overall [36]. However, Thomas et al. [37] indicated that this reaction is shown in

zero order with respect to the concentration of H_2O_2 in solutions containing a small amount of H_2O_2. In this work, the reaction was also considered in zero order with H_2O_2. The results of the experiments and modeling of the oxidation reaction of NO in the presence of H_2O_2 are compared in Fig. 6. The NO oxidation in the presence of H_2O_2 showed a higher conversion of NO than in the presence of water. However, there was no conversion difference for the 1% and 3% H_2O_2 baths at the same volume, flow rate, and O_2 concentration.

The predicted and experimental results differ with respect to the effect of the flow rate within a certain range of flowrate (i.e. <1 L/min) because of the formation of larger bubbles and the coalescence of bubbles caused in the system. The low flow rate increased the residence time but decreased the gas-liquid interfacial area [38]. Additional modifications reflecting the flow model might be required, but have not been considered in this research because such low flowrate is generally not considered for actual SMV operation.

3-3. Results of Parameter Estimation

The MATLAB optimization tool was used (Table 6 and Fig. 7) to yield optimal parameters for the kinetic model. It is a nonlinear problem; thus, the optimization was performed with the f_{solve} function of the optimization tool, which is nonlinear system solver. The f_{solve} function has three algorithms for optimization: trust region dogleg, trust region reflective, and Levenberg-Marquardt. The Levenberg-Marquardt algorithm was used because it has a greater stability and provides prompt results to find the optimal value compared to other algorithms [39]. This method might not be proper to find a global minimum point because the objective functions might have several local optimum points. However, we restricted the operating conditions of the model to meet the condition for field applications. Therefore, the Levenberg-Marquardt algorithm was considered to be appropriate enough to evaluate the validity and parameters with good initial values.

Table 6 shows the estimated parameters, from which the initial values were obtained in the section "Mathematical Modeling." The results of the parameter estimation did not deviate significantly from the literature. Parity plots were drawn using MATLAB to compare the estimated parameters with the initial values (Fig. 7). The experimental results were more consistent with the predicted results for the data shown in Fig. 7(b) than that in Fig. 7(a), which supports the validity of the parameter estimation. Lastly, the tendency for NO oxidation under various operating conditions is shown in Fig. 8. It shows the final modeling results for liquid-phase reaction with respect to the O_2 concentration, volume of the bath, flow rate (gas velocity), H_2O_2 concentration, and pH value. It is illustrated as 3D diagrams for understanding, which has the same tendency as the results of Fig. 6. The graphs of Fig. 8(a) and (b) show the NO conversion with respect to the volume of the bath and flow rate, and to the O_2 concentration and flow rate, respectively. The NO conversion with respect to the pH value and H_2O_2 concentration of the bath is exhibited in Fig. 8(c). These are more consistent with the experimental results than the before parame-

Table 6. Parameter estimation results for modeling

Parameter	Value	Unit	Parameter	Value	Unit
$K_{3,g}$	3.480E-04	$L\cdot mol^{-1}$	$(k_GA_G/V)_{NO}$	1.000E-03	s^{-1}
$K_{4,g}$	1.240E+01	$L\cdot mol^{-1}$	$(k_GA_G/V)_{O_2}$	1.000E-03	s^{-1}
$K_{5,g}$	1.660E+05	$L\cdot mol^{-1}$	$k_{H_2O_2}$	4.650E-02	s^{-1}
$k_{6,g}$	6.200E-03	s^{-1}	k (pH 1.5)	6.720E+06	$L^2\cdot mol^{-2}\cdot s^{-1}$
$k_{7,g}$	2.960E+07	$L\cdot mol^{-1}\cdot s^{-1}$	k (pH 3)	6.063E+06	$L^2\cdot mol^{-2}\cdot s^{-1}$
$k_{1,l}$	2.284E+06	$L^2\cdot mol^{-2}\cdot s^{-1}$	k (pH 7)	2.284E+06	$L^2\cdot mol^{-2}\cdot s^{-1}$
$k_{2,l}$	1.077E+09	$L\cdot mol^{-1}\cdot s^{-1}$	k (pH 12)	2.247E+06	$L^2\cdot mol^{-2}\cdot s^{-1}$
$k_{3,l}$	3.700E+04	s^{-1}			
$k_{4,l}$	1.110E+03	s^{-1}			

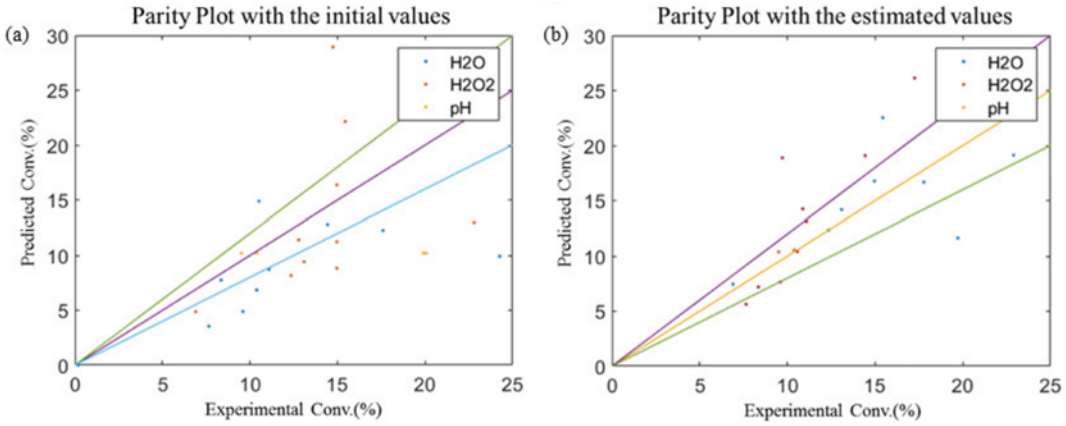

Fig. 7. Parity plots: (a) Initial values and (b) Estimated values.

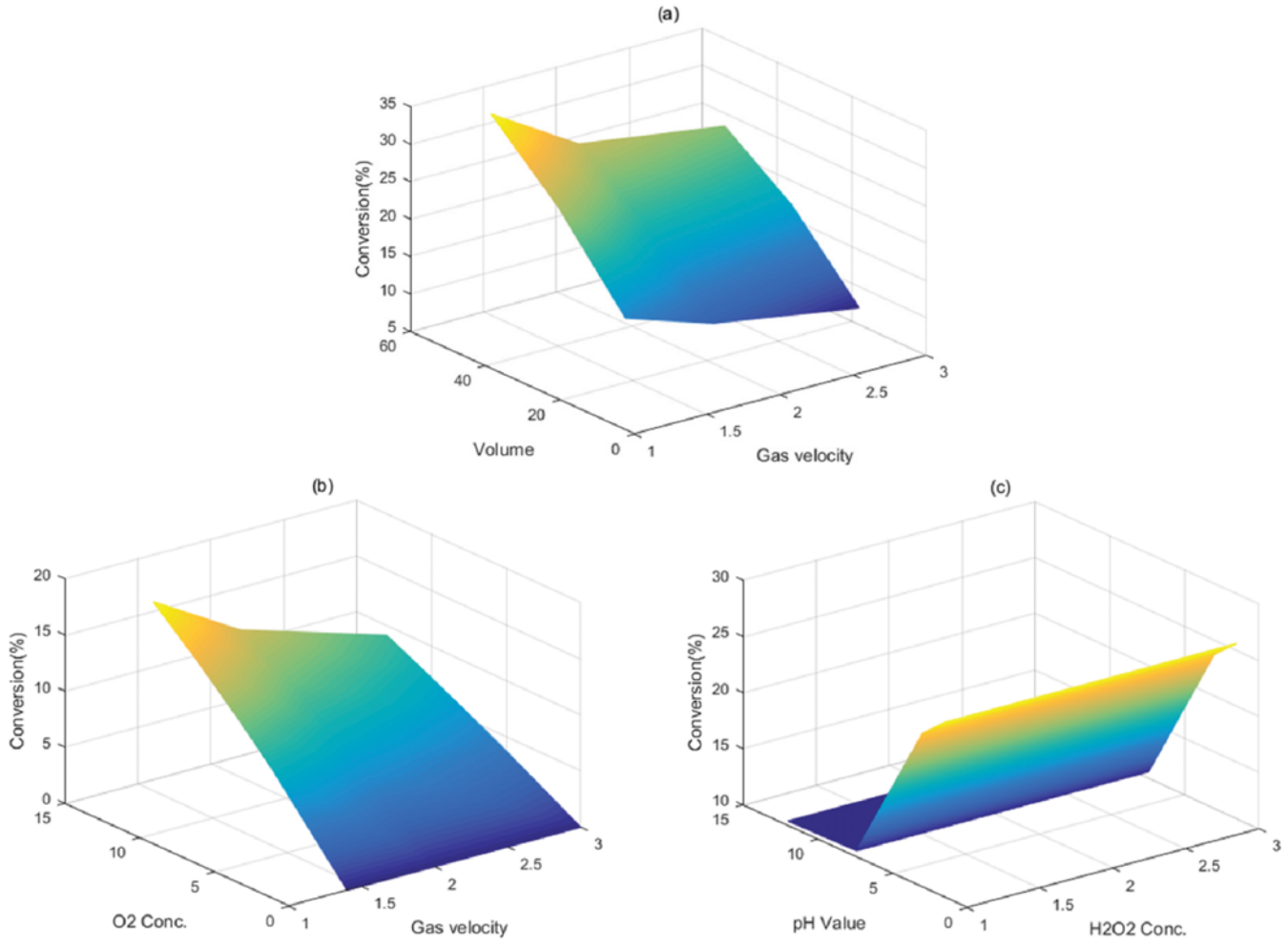

Fig. 8. (a) Effect of the gas velocity and volume of the bath, (b) Effect of the gas velocity and O_2 concentration, and (c) Effect of the pH and H_2O_2 concentration.

ter estimation. Therefore, the model results are reliable enough to predict the properties of the system.

CONCLUSION

We developed a new method to reduce NOx from the SMV flue gas further with minimum modification of the existing system. For this, reaction mechanism and kinetics were investigated through experiment, and a mathematical model of the system was developed based on the experiment results in this research.

For the oxidation of NO to NO_2, we conducted two separate experiments in gas and aqueous phases. In gas phase, nitric oxide is rarely converted to NO_2, regardless of the operating conditions (e.g., presence of water vapor, temperature, flow rate, and initial concentrations of NO and O_2). Even though the NO oxidation reaction has a high equilibrium conversion, it is considered that this result comes from the short residence time and the reduction of the reaction rate by a small amount of NO. We found that in this system, injecting additional oxygen and air to the exhaust gas, discharged from the burner, did not have a significant effect on NOx removal.

In the absorption experiments, namely, the liquid-phase reaction of NO, the following aspects were observed.

- The experimental results exhibited a tendency to increase the NO conversion as the flow rate was reduced, or the initial concentration of NO or O_2 was increased.
- At oxygen concentrations of 10% or greater, the NO conversion did not change significantly with increasing oxygen concentrations. There are expected economic and efficiency limitations if additional NO conversion is required by injecting only additional air or oxygen into the system.
- The conversion of NO in the H_2O_2 bath was approximately 1.3-times higher than that in the water bath without H_2O_2. In particular, the NO was partially converted to NO_2 in the H_2O_2 bath in the absence of oxygen, which shows that H_2O_2 reacts directly with nitric oxide. There was little change in the conversion of NO in the water bath in the presence of ≥10% O_2, and the conversion rate increased relatively linearly when the oxygen concentration increased in the H_2O_2 bath.
- The experimental results for the effects of pH indicated that a high conversion occurred at low pH. A low pH in the H_2O_2 bath increased the NO conversion by up to 23% at a NO concentra-

tion of 50 ppm.

The modeling results for the liquid-phase reaction also indicated that the NO conversions in the water bath and H_2O_2 bath increased with respect to the O_2 concentration and volume of the bath, but the conversion decreased with respect to the flow rate. For the change of flowrate, the modeling results deviated from the experimental results in the range of low flow rate because of the effect of bubbles. However, such low flowrate is not applicable to field applications because it must not lose its function as a heat exchanger. For this reason, the modeling results are reliable enough to predict the final NOx amount from the SMV system. This model was established based on the mechanisms and kinetics from the literature, enabling prediction of the actual experimental system. In addition, parameters of the model were adjusted to achieve high accuracy of the simulation results. For the optimization algorithm, we adopted the Levenberg-Marquardt in the research.

Based on the experimental and modeling results, the feasibility and availability for field applications were examined prior to the demonstration study of an actual SMV by injecting additional air or oxygen into the system, using a 1-3% H_2O_2 solution bath instead of a conventional water bath, and controlling the pH. This approach can be directly used without significant changes to the operating conditions of the existing SMV system, which makes it possible to deal with the strict environmental regulations for NOx, discharged from the stack while not losing its inherent function as a heat exchanger. In this regard, the modified process can be easily applicable to field without high economic burdens, including additional capital and operating costs.

ACKNOWLEDGEMENTS

This work was supported by Korea Gas Corporation and a research project of the Development of Integrated Interactive Model for Subsea and Topside System to Evaluate the Process Design of Offshore Platform, funded by the Ministry of Trade (project No. 10060099).

REFERENCES

1. NIER, National Air Pollutants Emission 2012, 11-1480523-002293-01, Ministry of Environment, Korea (2012).
2. Z. Guan, J. Ren, D. Chen, L. Hong, F. Li, D. Wang, Y. Ouyang and Y. Gao, *Korean J. Chem. Eng.*, **33**, 3102 (2016).
3. S. Egashira, *Kobelco Technol. Rev.*, **32**, 64 (2013).
4. K. Lee, *Appl. Chem. Eng.*, **21**, 243 (2010).
5. M. E. Morrison, R. G. Rinker and W. H. Corcoran, *Ind. Eng. Chem. Fundam.*, **5**, 175 (1966).
6. H. Tsukahara, T. Ishida and M. Mayumi., *Nitric Oxide*, **3**, 191 (1999).
7. M. Bodenstein and L. Wachenheim, *Z. Elektrochem.*, **24**, 183 (1918).
8. C. F. H. Tipper and R. K. Williams, *Trans. Faraday Soc.*, **57**, 79 (1961).
9. J. C. Treacy and F. Daniels, *J. Am. Chem. Soc.*, **77**, 2033 (1955).
10. J. Mahenc, G. Clot and R. Bes, *Bull. Soc. Chim. Fr.*, **5**, 1578 (1971).
11. I. C. Hisatsune and L. Zafonte, *J. Phys. Chem.*, **73**, 2980 (1969).
12. J. Olbregts, *Int. J. Chem. Kinet.*, **17**, 835 (1985).
13. J. H. Smith, *J. Am. Chem. Soc.*, **65**, 74 (1943).
14. R. Cueto and W. A. Pryor, *Vib. Spectrosc.*, **7**, 97 (1994).
15. F. B. Brown and R. H. Crist, *J. Chem. Phys.*, **9**, 840 (1941).
16. J. D. Greig and P. G. Hall, *Trans. Faraday. Soc.*, **63**, 655 (1967).
17. J. D. Greig and P. G. Hall, *Trans. Faraday. Soc.*, **62**, 652 (1966).
18. A. Aida, K. Miyamoto, S. Saito, T. Nakano, M. Nishimura, Y. Kawakami, Y. Omori, S. Ando, T. Ichida and Y. Ishibe, *Nihon Kyobu Shikkan Gakkai Zasshi*, **33**, 306 (1995).
19. D. H. Stedman and H. Niki, *J. Phys. Chem.*, **77**, 2604 (1973).
20. J. J. Bufalini and E. R. Stephens, *Int. J. Air Water. Poll.*, **9**, 123 (1965).
21. W. A. Glasson and C. S. Tuesday, *J. Am. Chem. Soc.*, **85**, 2901 (1963).
22. V. L. Pogrebnaya, A. P. Usov, A. V. Baranov, A. I. Nesterenko and P. I. Bez'yazychnyi, *Zh. Prikl. Khim.*, **48**, 954 (1975).
23. R. S. Lewis and W. M. Deen, *Chem. Res. Toxicol.*, **7**, 568 (1994).
24. D. A. Wink, J. F. Darbyshire, R. W. Nims, J. E. Saavedra and P. C. Ford, *Chem. Res. Toxicol.*, **6**, 23 (1993).
25. H. H. Awad and D. M. Stanbury, *Int. J. Chem. Kinet.*, **25**, 375 (1993).
26. X. L. Long, Z. L. Xin, M. B. Chen, W. Li, W. D. Xiao and W. K. Yuan, *Sep. Purif. Technol.*, **58**, 328 (2008).
27. D. S. Jin, B. R. Deshwal, Y. S. Park and H. K. Lee, *J. Hazard. Mater. B*, **135**, 412 (2006).
28. J. M. Kasper, C. A. Clausen III and C. D. Cooper, *J. Air Waste Manage. Assoc.*, **46**, 127 (1996).
29. A. D. Bhanarkar, R. K. Gupta, R. B. Biniwale and S. M. Tamhane, *Int. J. Environ. Sci. Technol.*, **11**, 1537 (2014).
30. D. Thomas and J. Vanderschuren, *Ind. Eng. Chem. Res.*, **36**, 3315 (1997).
31. D. Thomas and J. Vanderschuren, *Sep. Purif. Technol.*, **18**, 37 (1999).
32. S. E. Schwartz and W. H. White, *Adv. Environ. Sci. Eng.*, **4**, 1 (1981).
33. S. Park, Y. Lee, G. Kim and S. Hwang, *Korean J. Chem. Eng.*, **33**, 3417 (2016).
34. J. Kuropka, *Environ. Prot. Eng.*, **37**, 13 (2011).
35. M. Pires, M. J. Rossi and D. S. Ross, *Int. J. Chem. Kinet.*, **26**, 1207 (1994).
36. K. K. Baveja, D. S. Rao and M. K. Sarkar, *J. Chem. Eng. Jpn.*, **12**, 322 (1979).
37. D. Thomas and J. Vanderschuren, *Chem. Eng. Sci.*, **51**, 2649 (1996).
38. T. Wang and J. Wang, *Chem. Eng. Sci.*, **62**, 7107 (2007).
39. H. Lee, S. Lee, S. Hwang and D. Jin, *Korean Chem. Eng. Res.*, **54**, 340 (2016).